



Molecular Crystals and Liquid Crystals

Publication details, including instructions for authors and subscription information:

<http://www.tandfonline.com/loi/gmcl20>

Synthesis, Structure, and Magnetic Properties of [Dithiazolylum]_x[M(tdas)₂] Salts

Sarah S. Staniland^a, Wataru Fujita^b, Yoshikatsu Umezono^b, Kunio Awaga^b, Stephen Crawford^a, Simon Parsons^a & Neil Robertson^a

^a School of Chemistry, University of Edinburgh, Edinburgh, U.K.

^b Department of Chemistry, Graduate School of Science, Nagoya University, Nagoya, Japan

Version of record first published: 31 Aug 2006

To cite this article: Sarah S. Staniland, Wataru Fujita, Yoshikatsu Umezono, Kunio Awaga, Stephen Crawford, Simon Parsons & Neil Robertson (2006): Synthesis, Structure, and Magnetic Properties of [Dithiazolylum]_x[M(tdas)₂] Salts, *Molecular Crystals and Liquid Crystals*, 452:1, 123-135

To link to this article: <http://dx.doi.org/10.1080/15421400500377677>

PLEASE SCROLL DOWN FOR ARTICLE

Full terms and conditions of use: <http://www.tandfonline.com/page/terms-and-conditions>

This article may be used for research, teaching, and private study purposes. Any substantial or systematic reproduction, redistribution, reselling, loan,

sub-licensing, systematic supply, or distribution in any form to anyone is expressly forbidden.

The publisher does not give any warranty express or implied or make any representation that the contents will be complete or accurate or up to date. The accuracy of any instructions, formulae, and drug doses should be independently verified with primary sources. The publisher shall not be liable for any loss, actions, claims, proceedings, demand, or costs or damages whatsoever or howsoever caused arising directly or indirectly in connection with or arising out of the use of this material.



Synthesis, Structure, and Magnetic Properties of [Dithiazolylium]_x[M(tdas)₂] Salts

Sarah S. Staniland

School of Chemistry, University of Edinburgh, Edinburgh, U.K.

Wataru Fujita

Yoshikatsu Umezono

Kunio Awaga

Department of Chemistry, Graduate School of Science,
Nagoya University, Nagoya, Japan

Stephen Crawford

Simon Parsons

Neil Robertson

School of Chemistry, University of Edinburgh, Edinburgh, U.K.

Three new [dithiazolylium]_x[M(tdas)₂] salts are reported (tdas = 1,2,5-thiadiazole-3,4-dithiole). Single-crystal X-ray structures have been obtained for [BDTA]₂[Fe(tdas)₂Cl] (1) and [BDTA]₂[Ni(tdas)₂] (2) (BDTA = benzo-1,3,2-dithiazolyl). These are the first examples of integrated anion-cation stacking motifs for [M(tdas)₂]^{x-} complexes, as well as the first example of a nondimerized [Fe(tdas)₂]⁻ material. [BBDTA][Fe(tdas)₂] (3) (BBDTA = benzo-bis-1,3,2-dithiazolyl) is also reported, and the magnetic properties of (1) and (3) have been analyzed, showing (1) to be paramagnetic and (3) to have a mixture of dimer and Curie–Weiss behaviour.

Keywords: BBDTA; BDTA; crystal structure; dithiazolyl; metal-bis-dithiolene; tdas

INTRODUCTION

Metal bis-1,2-dithiolenes are sulfur-rich complexes that typically possess square-planar, electronically conjugated systems. These have yielded materials with many interesting properties such as

Address correspondence to Sarah S. Staniland, School of Chemistry, University of Edinburgh, West Mains Road, Edinburgh EH9 3JJ, U.K. E-mail: S.S.Staniland@ed.ac.uk

superconductivity [1], metallic and magnetic behavior [2], and non-linear optical properties [3]. These properties can be attributed to the extensive electronic delocalization of the HOMO and LUMO over the complex as well as longer-ranging electronic interactions through the material by extensive intermolecular overlap facilitated by the large π -orbitals of the sulfur atoms. Electronic bulk properties are readily seen in dithiolene complexes because of the propensity of the planar complexes to form stacking structures with intermolecular interactions in the stacking direction [2].

The bis-dithiolene ligand (tdas) (tdas = 1,2,5-thiadiazole-3,4-dithiole) was first synthesised 18 years ago because of the potential of $[M(\text{tdas})_2]^{x-}$ complexes to be candidate anions for new electronically correlated molecular materials. There is a close structural relationship of (tdas) to (dmit) (dmit = 1,3-dithiol-2-thione-4,5-dithiolate), used to prepare numerous $[M(\text{dmit})]^{x-}$ materials found to be conducting, superconducting, and magnetic. There is the added advantage that the (tdas) ligand is easily synthesised in a one-pot reaction.

Unfortunately however, open-shell $[M(\text{tdas})_2]^{x-}$ materials have generally yielded dimerized $[M(\text{tdas})_2]^{x-}$ complexes within the crystal structure, with a strong intermolecular M...S dimeric interaction, leading to generally unremarkable antiferromagnetic dimer behaviour. There is one exception: $[\text{BEDT-TTF}][\text{Ni}(\text{tdas})_2]^{4-}$, which was recently reported to have a structure of two-dimensional (2D) alternating layers of $[\text{BEDT-TTF}]$ dimers separated by isolated $[\text{Ni}(\text{tdas})_2]^{-}$ complexes and a layer of $[\text{Ni}(\text{tdas})_2]^{-}$ complexes arranged in a side-by-side ribbon motif. Although this structure shows that open-shell $[M(\text{tdas})_2]^{x-}$ complexes can crystallize in a nondimeric form, the $[\text{Ni}(\text{tdas})_2]^{-}$ units do not form a stacking motif [4], and it is stacking motif that is conducive to electronic communication that leads to electronic correlations through the material.

The three materials reported herein are salts with the $[M(\text{tdas})_2]^{x-}$ anion and a dithiazolylum cation. Dithiazolylum cations are composed of extensive planar phenyl and N,S-heterocyclic rings fused together. These are ideal cations for the formation of salts with extended electronic properties because they are planar, conjugated, sulfur rich, and delocalized, forming strong intermolecular π - π interactions [5].

Dithiazolyls and the greater family that includes dithiadithiazolyls have been studied extensively, because members of this family form materials that are celebrated as some of the first organic ferromagnets, including the magnetic material with the highest ordering temperature of any organic magnet (36 K) [6].

The materials in this study are composed of $[M(\text{tdas})_2]^{x-}$ cocrystallized with the dithiazolylum cations $[\text{BDTA}]^{+}$ and the dithiazolylum

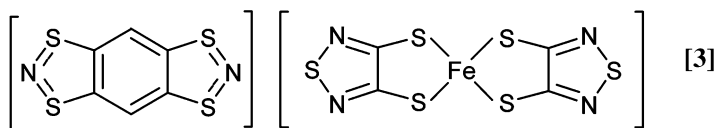
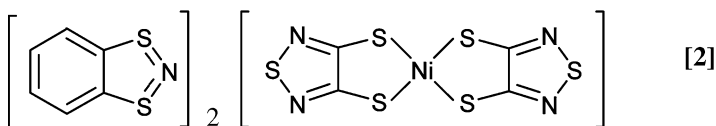
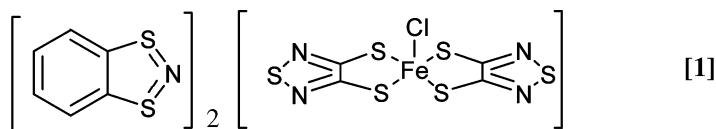


FIGURE 1 [BDTA]₂[Fe(tdas)₂Cl] (**1**), [BDTA]₂[Ni(tdas)₂] (**2**), and [BBDTA][Fe(tdas)₂] (**3**).

radical cation [BBDTA]⁺ (Fig. 1) (BDTA = benzo-1,3,2-dithiazolyl and BBDTA = benzo-bis-1,3,2-dithiazolyl). Both of these cations have displayed interesting magnetic properties. For example, [BDTA] can exist as a dimerized diamagnetic radical at room temperature and a paramagnetic liquid above 346 K; then above 360 K a double melt occurs that on cooling returns it to a paramagnetic solid, with antiferromagnetic ordering at 11 K [7]. The [BDTA]⁺ cation has previously been cocrystallized with metal-bis-dithiolene anions [8–10] to yield interesting new materials that have shown the cation to propagate magnetic interactions [8] as well as carry a partial charge, behaving as an open-shell conducting cation [10]. [BBDTA]⁺ has shown interesting magnetic behavior as a stable radical, and it has been cocrystallized to form the organic ferromagnet [BBDTA][GaCl₄] with an ordering temperature of 6.7 K [11].

Here we report the structures and magnetic properties of two new [BDTA]_x[M(tdas)₂] salts, [BDTA]₂[Fe(tdas)₂Cl] (**1**) and [BDTA]₂[Ni(tdas)₂] (**2**) (Fig. 1) that display integrated anion-cation alternating stacks, the ideal motif for the formation of new functional materials. The [Fe(tdas)₂Cl]^{2−} complex is an open-shell radical anion and is the first example of an integrated-stack motif for an [Fe(tdas)₂][−] salt. We also report the synthesis and magnetic properties of [BBDTA][Fe(tdas)₂] (**3**) (Fig. 1), which appears to show hybrid magnetic character.

EXPERIMENTAL

Synthesis

[BDTA][Cl] [12], [BBDTA][FeCl₄] [13,14], [TBA]₂[Ni(tdas)₂] [15], and [TBA][Fe(tdas)₂] [15] were synthesised by literature methods.

Single crystals of [BDTA]₂[Fe(tdas)₂Cl] (**1**) were obtained by layering [BDTA][Cl] in THF on top of [TBA][Fe(tdas)₂] in DCM and allowing it to diffuse. After 40 days, small, dark, rectangular-shaped crystals were collected.

Single crystals of [BDTA]₂[Ni(tdas)₂] (**2**) were obtained by layering [BDTA][Cl] in MeCN on top of [TBA]₂[Ni(tdas)₂] in DCM and allowing it to diffuse. After 23 days, small, dark, needle-shaped crystals were collected. The microcrystalline bulk samples of both (**1**) and (**2**) were washed with MeCN and ether and analyzed by CHN and X-ray powder diffraction to establish that the bulk samples possessed the same composition and phase as the single crystals used to determine the structures.

[BBDTA][Fe(tdas)₂] (**3**) was prepared by adding a solution of [BBDTA][FeCl₄]·MeCN to a solution of [TBA][Fe(tdas)₂] dissolved in MeCN and stirring. A dark precipitate formed almost instantly, and this was washed with MeCN and ether and analyzed by CHN and X-ray powder diffraction to confirm that the sample was crystalline. The bulk samples of (**1**)–(**3**) were then used for the magnetic measurements.

CHN Analysis

[BDTA]₂[Fe(tdas)₂Cl] (**1**)

C₁₆H₈ClFeN₆S₁₀. Calculated: C, 27.60; H, 1.16; N, 12.07. Found: C, 30.36; H, 1.48; N, 11.58%.

[BDTA]₂[Ni(tdas)₂] (**2**)

C₁₆H₈N₆NiS₁₀. Calculated: C, 28.96; H, 1.22; N, 12.66. Found: C, 28.74; H, 0.98; N, 12.62%.

[BBDTA][Fe(tdas)₂] (**3**)

C₁₀H₂FeN₆S₁₀. Calculated: C, 20.61; H, 0.35; N, 14.78. Found: C, 20.64; H, 0.10; N, 14.60%.

X-ray Crystallography Data

Diffraction data for both samples were collected with Mo-K α radiation on a Bruker Smart Apex CCD diffractometer equipped with an Oxford Cryosystems low-temperature device at 150 K. Absorption corrections were applied using the multiscan procedure SADABS [16]. The structures were solved by Patterson methods (DIRDIF) [17] and refined by

full-matrix least squares against $|F|^2$ using all data (CRYSTALS) [18]. Crystallographic information files have been deposited with the Cambridge Crystallographic Database for (1) and (2) with the reference codes CCDC 281554 and 281555, respectively.

[BDTA]₂[Fe(tdas)₂Cl] (1)

C₁₆H₈ClFeN₆S₁₀; M = 696.24; monoclinic; $a = 7.273$, $b = 13.969$, $c = 12.282$ Å; $\alpha = 90$, $\beta = 95.14$, $\gamma = 90^\circ$; $U = 1242.84(8)$ Å³; $T = 150$ K; space group Pn ; $Z = 2$, $\mu(\text{Mo-K}\alpha) = 0.7107$ mm⁻¹; 5914 reflections were collected, 5914 reflections were independent; ($R_{\text{int}} = 0.022$); these were used in all calculations.

The Fe complex is disordered about a pseudo-inversion center. The major components consist of Fe1, Cl1, and ligands S11-S71 and S12-S71; the minor components consist of Fe2, Cl2, and ligands S111-S171 and S112-S171. The occupancies were 0.8602(14) and 0.1398(14). The two BDTA cations are also related by the pseudo-inversion symmetry.

Had the occupancies of the disordered components of the complex both been 0.5, the space group would have been $P2_1/n$. There is an ambiguity between space groups $P2/n$ and Pn because both give rise to the same set of systematic absences. However, the location of the pseudo-inversion center at ca. $1/4$ of a unit cell translation along y from the n -glide shows that $P2/n$ is not a suitable space group in the case of this structure (in $P2/n$ the inversion center is coincident with the glide plane). The value of $\langle I/u(I) \rangle$ for the $0k0$ reflections with $k = 2n + 1$ was 11.4, clearly ruling out $P2_1/n$. Additionally, an attempt to model the structure in $P2_1/n$ yielded $R1 = 13.32\%$ for 2944 $|F_0| > 4u(|F_0|)$ and 13.57% for all 3073 data and 164 parameters (SHELXL-97) [19].

Although the occupancies of the disorder deviate from the pseudo-inversion symmetry, the relationship between positional parameters is obeyed much more closely. To make this clearer, the structure was refined in a nonstandard setting of Pn with the n -glide at $y = 1/4$ and the pseudo center at the origin.

The structure was initially modelled with the Fe and Cl atoms split over two sites and two fully occupied (tdas) ligands. Free refinement yielded Fe-S distances in the range 1.9–2.3 and S-Fe-Cl angles in the range 82–119°. These were interpreted as the consequences of ill-conditioning of the least squares by the pseudo-inversion symmetry, and the refinement strategy adopted followed the recommendations of Watkin [20] and Prince [21]. Hence, the least squares was parameterized with the sums and differences of inversion-related parameters: for example, rather than refine $S(11,x)$ and $S(12,x)$, the quantities $[S(11,x) + S(12,x)]$ and $[S(11,x) - S(12,x)]$ were refined instead.

Common anisotropic displacement parameters were refined for atoms related by the pseudo-inversion center. Similarity restraints were applied to related bond distances and angles in chemically similar ligands. Similarity restraints were also applied to the Fe-S and Cl...S distances in the complex anion. The Flack parameter was included in the full-matrix least squares.

$R1$ [based on data with $|F_0| > 4u(|F_0|)$] converged to 6.37%. Though this is a clear improvement over the centrosymmetric model, it was necessary to use very large weights for the Fe-S and Cl...S similarity restraints (s.u. = 0.001 Å) to obtain a model with an acceptable variation in these distances. The similarity restraints were therefore removed from the distances involving Fe2 and Cl2. Equivalent adps were assigned to S(11) and S(111) and so on. After a few cycles of refinement, the disorder was extended to the (tdas) ligands by generating alternative sites with the pseudo-inversion center. The minor weight ligands were treated as rigid groups, and similarity restraints reapplied to all Fe-S and S...Cl distances. The refinement converged to $R1 = 3.8\%$ within a few cycles.

[BDTA]₂[Ni(tdac)₂] (2)

C₁₆H₈N₆NiS₁₀; $M = 663.65$, monoclinic; $a = 10.9893(11)$, $b = 9.1344(9)$, $c = 11.3177(11)$ Å; $\alpha = 90$, $\beta = 101.8420(10)$, $\gamma = 90^\circ$; $U = 1111.90(19)$ Å³; $T = 150$ K; space group $P2_1/n$; $Z = 2$; $\mu(\text{Mo-K}\alpha) = 0.7107 \text{ mm}^{-1}$, 7031 reflections were measured, 2676 independent reflections ($R_{\text{int}} = 0.027$), which were used in all calculations. The final $wR(F^2)$ was 0.0727.

Magnetic Susceptibility

Magnetic susceptibility measurements were performed on the micro-crystalline samples (1)–(3) from 300–2 K using a Quantum design MPMS₂ SQUID magnetometer with MPMS MultiVu application software to process the data. A variable field measurement was performed from 0 to 5 T at 2 K to ensure that the magnetic results were linearly dependent on field. The magnetic field used for the variable temperature measurements was 0.1 T.

RESULTS AND DISCUSSION

Crystal Structures

Crystal Structure of [BDTA]₂[Fe(tdac)₂Cl] (1)

The salt (1) crystallizes in a 2:1 stoichiometry of [BDTA]⁺ to [Fe(tdac)₂Cl]²⁻. The four-coordinate iron center is pyramidal as it is

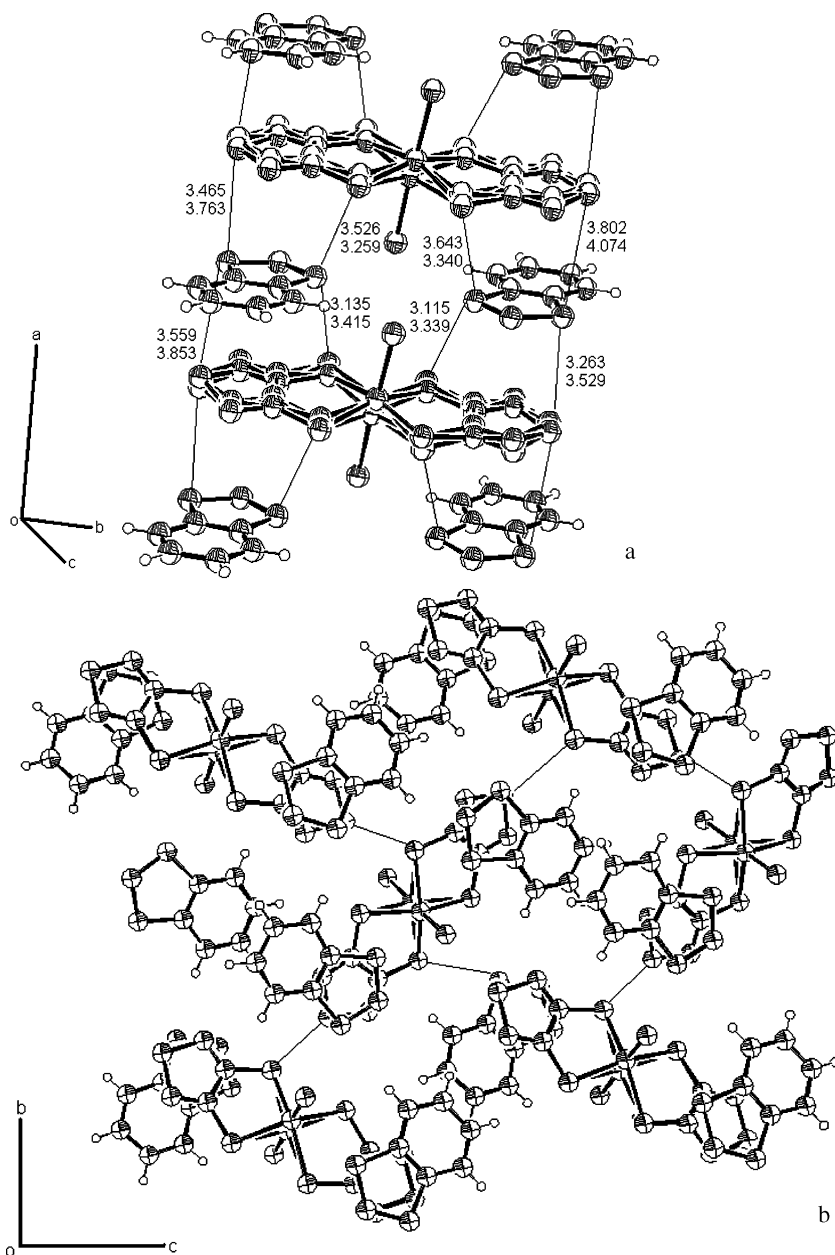


FIGURE 2 Crystal structure drawn in Ortep of (1) viewed (a) perpendicular to the a-axis showing the stacking motif and (b) down the a-axis. Interatomic distances are shown in 2a as two values due to disorder. Interatomic distances in 2b are 3.208–3.730 Å.

puckered toward the chloride atom with an interatomic distance of 2.316 Å and can thus be considered bonding. There is an intrinsic disorder of the direction the $[\text{Fe}(\text{tdas})_2\text{Cl}]^{2-}$ anion faces. In keeping with related air-stable salts, the iron center can be considered to be Fe^{3+} and thus paramagnetic. This material possesses alternating stacks along the *a*-axis of $[\text{Fe}(\text{tdas})_2\text{Cl}]^{2-}$ units between pairs of $[\text{BDTA}]^+$ cations (Fig. 2a). The $[\text{BDTA}]^+$ anions stacked below, approximately at right angles to, and overlapping one side of the $[\text{Fe}(\text{tdas})_2\text{Cl}]^{2-}$, with the another, symmetry-related $[\text{BDTA}]^+$ molecule diagonally opposite and above the $[\text{Fe}(\text{tdas})_2\text{Cl}]^{2-}$ plane, forming a centrosymmetric stacking unit in a zigzag motif if viewed down the stack (Fig. 2b). Within the stacking direction, there are short contact distances between sulfur atoms on the cation and anion shown in Fig. 2a, and these are repeated down the stack. Most of these contacts are short enough to allow the possibility of π -orbital overlap and thus magnetic interactions through the stack. Between each stacking unit there are short contact distances from each terminal sulfur on $[\text{Fe}(\text{tdas})_2\text{Cl}]^{2-}$ to a metal-coordinated sulfur atom on an adjacent $[\text{Fe}(\text{tdas})_2\text{Cl}]^{2-}$ perpendicular to the first in the next stack. Each stack is tilted at an angle $\approx 31.4^\circ$ out of the *b*-*c* plane to display short contact distances in a diagonal 2D plane through the stacking system.

Thus, it can be said that the solid-state structure of $[\text{BDTA}]_2[\text{Fe}(\text{tdas})_2\text{Cl}]$ is composed of mixed alternating cation-anion stacks with short contacts through the stacks, as well as in three dimensions between each stacking unit. This solid-state structure is unique for a $[\text{M}(\text{tdas})_2]^{x-}$ system and potentially important for the design of new functional materials. The key features of this structure are the planar stacking motif with $[\text{Fe}(\text{tdas})_2]^-$ units that do not dimerize, and this is the first example of a nondimerized motif for an open-shell $[\text{Fe}(\text{tdas})_2]^-$ unit. These are important prerequisites for a novel magnetic or conducting lattice. The material can also be seen to have a mixed alternating anion-cation stack that has the potential to form a more diverse range of interesting functional materials.

Crystal Structure of $[\text{BDTA}]_2[\text{Ni}(\text{tdas})_2]$ (2)

Salt (2) could be crystallized in a range of different solvents and conditions to yield the 2:1 stoichiometric crystal structure shown in Fig. 3. This 2:1 stoichiometry yields a material with a metal center, which is diamagnetic.

The salt (2) crystallizes with a stacking motif along the *c*-axis. Each $[\text{BDTA}]_2[\text{Ni}(\text{tdas})_2]$ unit is tilted 23.12° out of the plane, perpendicular to the stacking axis, forming sheets of stacks, with alternate sheets tilted toward the *b*-axis and then away from the *b*-axis (this layer

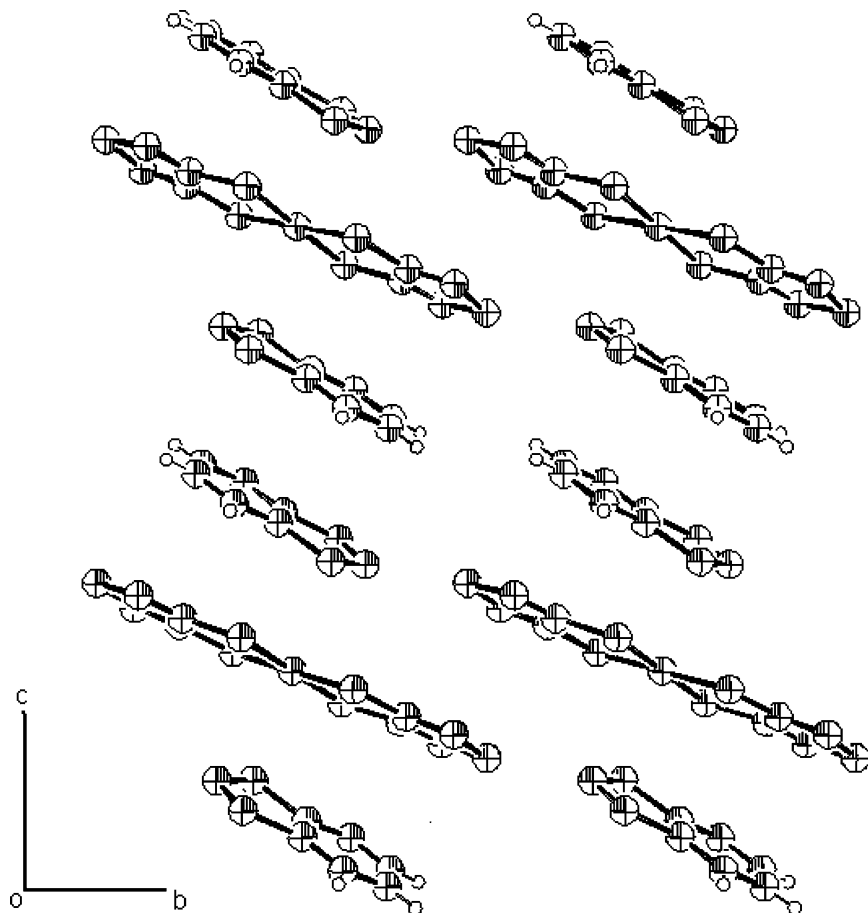


FIGURE 3 Crystal structure drawn in Ortep of (2) viewed along the *a*-axis.

not shown). There are short electrostatic interactions between the $[\text{Ni}(\text{tdas})_2]^{2-}$ anion and the $[\text{BDTA}]^+$ stacked above and below 2.852 \AA . There are two stacking $[\text{BDTA}]^+$ cations between each $[\text{Ni}(\text{tdas})_2]^{2-}$ anion, and these have an interplanar distance of 3.428 \AA . There is a $[\text{BDTA}]^+$ plane to the Ni-atom of $[\text{Ni}(\text{tdas})_2]^{2-}$ distance of 2.765 \AA . This forms a stack with intermolecular distances short enough for potential electronic correlations. Unfortunately, this system is diamagnetic; however, it is structurally significant, as out of the seven reported $[\text{Ni}(\text{tdas})_2]^{x-}$ structures, this is only the second to display an integrated cation-anion stacking motif [22], but the first to show a short intermolecular π -stacking distance with planar cations.

Magnetic Susceptibility

It can be surmised from the stoichiometry, and was then shown by magnetic measurement, that **(2)** is diamagnetic. However, variable temperature magnetic data were recorded for **(1)** and **(3)**, and the molar magnetic susceptibility calculated.

The molar magnetic susceptibility of **(1)** shows Curie–Weiss behavior over the entire temperature range with a Curie constant (C) of $1.50 \pm 0.011 \text{ emu K mol}^{-1}$ and a Weiss constant (θ) of $-0.95 \pm 0.021 \text{ K}$. The high temperature data were also fit to the Curie–Weiss model ($80 < T < 320 \text{ K}$) to eliminate any deviations from the model at low temperature due to any potential long-range ordering. Constants obtained were $C = 1.94 \pm 0.005 \text{ emu K mol}^{-1}$ and $\theta = -6.27 \pm 0.018 \text{ K}$. As the iron center is in an approximate square planar site, one can expect three unpaired electrons, as population of higher energy d-orbitals is lost in this configuration. This has been proven for the related salt $[\text{TBA}][\text{Fe}(\text{tdas})_2]$ by a combination of susceptibility and Mössbauer measurements [23]. Three unpaired electrons will give a theoretical spin-only Curie constant of $1.875 \text{ emu K mol}^{-1}$, which is in close agreement with the higher temperature experimental value. This, along with the small Weiss constant, reveals **(1)** to be a paramagnetic material with evidence of weak antiferromagnetic interactions although with any resulting ordering temperature too low to be seen in these data. This demonstrates that the integrated-stack structure of **(1)** leads to some intermolecular interaction and magnetic exchange. Despite observing only weak antiferromagnetic coupling, this behavior is nevertheless unique in comparison to all other $[\text{Fe}(\text{tdas})_2]^-$ materials, which show dimerized anions, and this gives the first suggestion that more interesting magnetic behavior in such salts could occur.

The magnetic data collected for **(3)** is more complex because of the inclusion of both radical cations, $[\text{BBDTA}]^+$, and radical anions, $[\text{Fe}(\text{tdas})_2]^-$. The curve obtained for molar magnetic susceptibility versus temperature plot does not conform to the Curie–Weiss model, and a $\chi_{\text{mol}}T$ versus temperature plot shows activated behavior that is indicative of strong magnetic interactions. Unfortunately, a crystal structure has not been obtained for this material, as large good quality crystals could not be obtained; however, X-ray powder diffraction has shown that **(3)** is microcrystalline. As both anion and cation are magnetic, it can be assumed that both ions contribute to the magnetism of **(3)**, displaying a mixed magnetic character.

All examples of $[\text{Fe}(\text{tdas})_2]^-$ (with the exception of **(1)**), have a crystal structure that has dimerized $[\text{Fe}(\text{tdas})_2]_2$ units. It is therefore

reasonable to assume in the absence of a crystal structure that the $[\text{Fe}(\text{tdac})_2]^-$ anions within (**3**) also dimerize with a strong coupling. Although the molar magnetic susceptibility curve cannot be modeled by a pure Curie–Weiss model, the shape suggests some Curie–Weiss character, and this could be contributed by a paramagnetic signal from the $[\text{BBDTA}]^+$ cation. This magnetic model can be tested by subtraction of a Curie component corresponding to the $[\text{BBDTA}]^+$ from the magnetic susceptibility data, and this plot is shown in Fig. 4. Here one can clearly see a peak due to strong antiferromagnetic coupling as would be anticipated through dimerization of the anions. This can be fitted to the Bleaney–Bower model [24] to give a predictably strong magnetic coupling of $J/k = -76 \pm 0.2$ K, which is comparable to the coupling of other literature examples of $[\text{Fe}(\text{tdac})_2]_2^{2-}$ dimers ($J/k = -108$) [25]. Thus, the suggested magnetic structure of (**3**) is a mixed model of a Curie–Weiss component to represent the noninteracting paramagnetic cation $[\text{BBDTA}]^+$ with $C = 0.375 \text{ emu K mol}^{-1}$, along with $[\text{Fe}(\text{tdac})_2]^-$ anions forming dimers with a strong antiferromagnetic coupling interaction with $J = -76$ K.

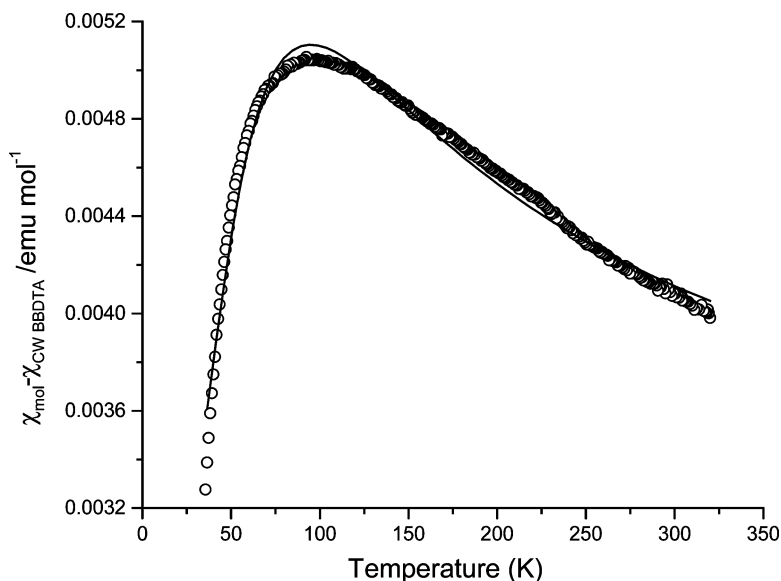


FIGURE 4 Molar magnetic susceptibility versus temperature (2–320 K) of (**3**) with a Curie component for $[\text{BBDTA}]^+$ subtracted ($C = 0.375$) (○). — = Bleaney–Bower fit for a dimer with $J/k = -76 \pm 0.2$ K.

CONCLUSION

Two [BDTA]₂[M(tdas)₂] salts have been synthesized and crystallized to give two structures with novel and useful motifs. Both have nondimerized stacking structures, which is beneficial for the design of new material with correlated electronic properties. The structure of **(1)** is the first example of an open-shell [Fe(tdas)₂][−] anion that does not form dimerized units within a structure. Both structures also have integrated anion-cation stacks, which can be useful for designing new functional materials with unusual and/or hybrid properties. The magnetic properties of **(1)** show it to be a Curie–Weiss paramagnet with $C = 1.94 \text{ emu K mol}^{-1}$ and $\theta = -6.27 \text{ K}$ with no antiferromagnetic ordering occurring above 2 K. Although no structural information has been obtained for **(3)**, it has shown mixed magnetic properties attributed to a Curie–Weiss contribution from the radical cation and an antiferromagnetic dimerization of the anion with a coupling of -76 K . Although, the magnetic properties of these materials do not display particularly novel characteristics, they clearly illustrate the potential of [dithiazolylum]_x[M(tdas)₂] salts to form novel magnetic materials as they demonstrate the appropriate stacking motifs that lead to intermolecular magnetic exchange and hybrid magnetic properties.

REFERENCES

- [1] Cassoux, P. (1999). *Coord. Chem. Rev.*, 185–186, 213.
- [2] Robertson, N. & Cronin, L. (2002). *Coord. Chem. Rev.*, 227, 93.
- [3] Romaniello, P. & Leij, F. (2003). *Chem. Phys. Lett.*, 372, 51.
- [4] Curreli, S., Deplano, P., Mercuri, M. L., Pilia, L., Serpe, A., Schlueter, J. A., Whited, M. A., Geiser, U., Coronado, E., Gomez-Garcia, C. J., & Canadell, E. (2004). *Inorg. Chem.*, 43, 2049.
- [5] Rawson, J. M. & McManus, G. D. (1999). *Coord. Chem. Rev.*, 189, 135.
- [6] Banister, A. J., Bricklebank, N., Lavender, I., Rawson, J. M., Gregory, C. I., Tanner, B. K., Clegg, W., Elsegood, M. R. J., & Palacio, F. (1996). *Angew. Chem., Int. Ed. Engl.*, 35, 2533.
- [7] Fujita, W., Awaga, K., Nakazawa, Y., Saito, K., & Sorai, M. (2002). *Chem. Phys. Lett.*, 352, 348.
- [8] Staniland, S. S., Fujita, W., Yoshikatsu, U., Awaga, K., Camp, P. J., Clark, S. J., & Robertson, N. (2005). *Inorg. Chem.*, 44, 546.
- [9] Umezono, Y., Fujita, W., & Awaga, K. (2005). *Chem. Phys. Lett.*, 409, 139.
- [10] Staniland, S. S., Fujita, W., Umezono, Y., Awaga, K., Clark, S. J., Cui, H., Kobayashi, H., & Robertson, N. (2005). *J. Chem. Soc. Chem. Commun.*, 3204.
- [11] Fujita, W. & Awaga, K. (2002). *Chem. Phys. Lett.*, 357, 385.
- [12] Wolmershaeuser, G., Schnauber, M., & Wilhelm, T. (1984). *J. Chem. Soc. Chem. Commun.*, 573.
- [13] Wolmershaeuser, G., Wortmann, G., & Schnauber, M. (1988). *J. Chem. Res. Synop.*, 358.

- [14] Barclay, T. M., Cordes, A. W., de Laat, R. H., Goddard, J. D., Haddon, R. C., Jeter, D. Y., Mawhinney, R. C., Oakley, R. T., Palstra, T. T. M., Patenaude, G. W., Reed, R. W., & Westwood, N. P. C. (1997). *J. Am. Chem. Soc.*, **119**, 2633.
- [15] Hawkins, I. & Underhill, A. E. (1990). *J. Chem. Soc. Chem. Commun.*, 1593.
- [16] Sheldrick, G. M. (2004). University of Göttingen, Germany.
- [17] Beurskens, P. T., Beurskens, G., Bosman, W. P., de Gelder, R., Garcia Granda, S., Gould, R. O., Israel, R., & Smits, J. M. M. (1996). University of Nijmegen, Toernooiveld 1, 6525 ED Nijmegen, The Netherlands.
- [18] Betteridge, P. W., Carruthers, J. R., Cooper, R. I., Prout, K., & Watkin, D. J. (2003). *J. Appl. Crystallogr.*, **36**, 1487.
- [19] Sheldrick, G. M. (1997). University of Göttingen, Germany.
- [20] Watkin, D. (1994). *Acta Crystallogr. Sect. A: Found. Crystallogr.*, **A50**, 411.
- [21] Prince, E. (1994). *Mathematical techniques in crystallography and materials science*. Springer: Berlin.
- [22] Okuno, T., Kuwamoto, K., Fujita, W., Awaga, K., & Nakanishi, W. (2003). *Polyhedron*, **22**, 2311.
- [23] Takahashi, M., Takeda, M., Awaga, J., Okuno, T., Maruyama, Y., Kobayashi, A., Kobayashi, H., Schenk, S., Robertson, N., & Underhill, A. E. (1996). *Mol. Cryst. and Liq. Cryst. Section A: Mol. Cryst. and Liq. Cryst.*, **286**, 399.
- [24] Bleaney, B. & Bowers, K. D. (1952). *Proc. Roy. Soc. (London)*, **A214**, 451.
- [25] Awaga, K., Okuno, T., Maruyama, Y., Kobayashi, A., Kobayashi, H., Schenk, S., & Underhill, A. E. (1994). *Inorg. Chem.*, **33**, 5598.